Coordination Chemistry Reviews 255 (2011) 2810–2820

Contents lists available at ScienceDirect

Coordination Chemistry Reviews

journal homepage: www.elsevier.com/locate/ccr

Review

Pseudocontact shifts in lanthanide complexes with variable crystal field parameters

Sebastiano Di Pietro[a], Samuele Lo Piano[a,b], Lorenzo Di Bari[a,*]

[a] Dipartimento di Chimica e Chimica Industriale, Università di Pisa, Via Risorgimento 35, I-56126 Pisa, Italy
[b] Scuola Normale Superiore, Piazza Cavalieri 7, I-56126, Pisa, Italy

Contents

ARTICLE INFO

Article history:
Received 3 February 2011
Accepted 11 May 2011
Available online 17 May 2011

Keywords:
Pseudocontact shifts
Lanthanide complexes
Paramagnetic NMR

ABSTRACT

Accurate pseudocontact shifts are the basis for structural determination in solution by means of paramagnetic NMR. Separation of pseudocontact (PCS) from Fermi contact (FC) shifts from NMR data can be achieved by means of the so-called Reilley method, which is briefly critically reviewed. It encounters a relevant limitation in the case of change of crystal field parameters through the series, as determined by various processes, primarily axial ligand dynamics, or as a consequence of lanthanide contraction. We propose a simple alternative procedure to compensate for any variation (smooth or abrupt) in crystal field parameters. Four examples taken from the literature, plus the complete set of unpublished data for Ln DOTMA are discussed in detail to illustrate the power and limitation of the conventional Reilley treatment and to demonstrate the power and scope of our alternative approach.

1. Introduction

Paramagnetic NMR provides some of the most sensitive and accurate experimental parameters for structural determinations in solution [1,2]. Paramagnetism enhances relaxation rates and induces remarkable shift of nuclear resonances. This is true for both *d*- and *f*-metals, where the former have been very widely used in the context of biomolecular NMR [1], while the latter have widespread interest for small or medium-size molecules [3,4], although their use in proteins and nucleic acids is gaining increasing interest [5,6].

Owing to the very similar ionic radius and identical structure of the frontier orbitals, lanthanide(III) ions are usually considered to provide isostructural complexes throughout the series, possibly with a higher degree of homogeneity within the elements at the beginning or at the end of the series [7]. This fact is the basis for extracting contributions containing structural information from experimental observables, because one is able to compare the values of observables, measured on complexes having the same geometrical and electronic structure but different magnetic properties. A very relevant case is provided by the extraction of pseudocontact shifts (PCS), which are valuable pieces of geometrical information [8]. This is because they display a marked dependence on the polar coordinates of the observed nucleus in a reference system based on the magnetic anisotropy tensor. Thus, they offer the basis for accurate geometry determination in solu-

* Corresponding author. Tel.: +39 050 2219 298; fax: +39 050 2219 260.
E-mail address: ldb@dcci.unipi.it (L. Di Bari).

0010-8545/$ – see front matter © 2011 Elsevier B.V. All rights reserved.
doi:10.1016/j.ccr.2011.05.010

Table 1
C_{Ln}, $\langle S_z\rangle_{Ln}$ and their ratio.

	Ce	Pr	Nd	Sm	Eu	Tb	Dy	Ho	Er	Tm	Yb
C_{Ln}	−6.48	−11.41	−4.46	0.52	4.00	−86.84	−100.00	−39.25	32.40	52.53	21.64
$\langle S_z\rangle_{Ln}$	0.98	2.97	4.49	−0.06	−10.68	−31.82	−28.54	−22.63	−15.37	−8.21	−2.59
$C_{Ln}/\langle S_z\rangle_{Ln}$	−6.61	−3.84	−0.99	−8.68	−0.37	2.73	3.50	1.73	−2.11	−6.40	−8.36

C_{Ln} are recalculated according to Bleaney [17], except for Eu, whose value is taken from [19]; $\langle S_z\rangle_{Ln}$ is taken from [16]. The Sm value for $\langle S_z\rangle$ is affected by a high variability.

tion, provided they are reliably extracted from the observed shifts. To this end, Reilley developed a procedure, which is based on the conservation of crystal field parameters from one complex to another of the same ligand [9].

The existence of an exchangeable coordination site is a key feature for functional systems: molecular recognition [10], enantiomer discrimination [11], substrate activation [12], luminescence quenching [13], water nuclear relaxation (T_1-contrast in MRI) [14], and saturation transfer contrast enhancement [15] are all dependent on the dynamic binding of a ligand (most often water) to Ln^{3+}. As a consequence, most complexes are designed with a good chelating agent (often macrocyclic), leaving at least one position (hereafter called *axial*) open to dynamic coordination. This feature is associated with a variable coordination number (CN) along the series, whereby early lanthanides tend to bind ancillary ligands, which may be absent in the complexes of the late ions [16]. This has a negative effect on the separation of PCS because one cannot treat simultaneously data of complexes with different CN (usually before or after the so-called "gadolinium break") [17,18].

We shall develop a simple set of equations, directly derived from the standard Reilley treatment, for achieving the isolation of PCS, in cases with variable CN. We shall then see that the same treatment can be extended to other cases, where the properties of the main chelating agent are modulated, because of polarizability effects, as in heterobimetallic systems or because of a peculiar conformational feature, typical of DOTA derivatives. In all these cases, we shall see how can one take advantage of a large set of data and extract reliable PCS.

This alternative procedure for achieving separation of Fermi contact (FC) shifts from PCS is independent of crystal field parameters and provides reliable results even in cases of variable (possibly fractional) occupancy of the axial coordination site. It may be regarded as an extension of the "two nuclei" method [19], and its power resides in two points: (1) it is very straightforward to use and may be easily implemented on spreadsheets set up for the standard Reilley procedure and (2) it does not depend on the choice of nuclei nearby in the transition, but uses all the available set of experimental data. In its present form, our theory is addressed to complexes endowed with axial symmetry, i.e. containing a C_n-axis with $n \geq 3$. While we are currently working at systems with lower symmetry, where rhombic term cannot be neglected, we must observe that fast geometric rearrangements and ligand exchange often render *effective* axial symmetry much more common than expected [20,21].

2. Total paramagnetic shifts and pseudocontact shifts

The paramagnetic shift, δ^{para}, is defined as the difference between the observed shift, δ^{obs}, of a certain nucleus on a ligand in a paramagnetic complex and in a reference diamagnetic compound (δ^{dia}), which should have the same geometrical and electronic structures (from the ligand point of view) [2,3]. This is the first aspect which makes lanthanides unique: La^{3+} and Lu^{3+} are ideal standards for obtaining δ^{dia}, because they provide isostructural complexes for the early and the late elements of the series, respectively [3,4].

In turn, δ^{para} is the sum of two contributions: the Fermi contact shift, δ^{con} (abbreviated in the text as FC) and the pseudocontact shift, δ^{PC} (abbreviated in the text as PCS). As a result we can write for each NMR-active nucleus *i*:

$$\delta^{obs}(i) = \delta^{para}(i) + \delta^{dia}(i) = \delta^{con}(i) + \delta^{PC}(i) + \delta^{dia}(i) \quad (1)$$

Fermi contact is due to unpaired electron delocalization from the Ln^{3+}onto the nucleus *i* and is transmitted through bonds, very similarly to the usual *J*-coupling in diamagnetic NMR. It becomes negligibly small with the increasing number of bonds between Ln and *i*, although in the presence of conjugation it may propagate to a somewhat less predictable extent. The contact shifts for the nucleus *i* on a ligand in isostructural lanthanide complexes is proportional to the expectation values of S_z for that Ln^{3+} [22], which are known and tabulated (see Table 1)

$$\delta^{con}_{Ln}(i) = \langle S_z\rangle_{Ln} F(i) \quad (2)$$

$F(i)$ is a proportionality constant which depends solely on the specific nucleus *i*.

Pseudocontact shifts encode geometric information, hence their popularity in structural determination. For simplicity of algebraic arguments, in the following we shall consider only axially symmetrical species, i.e. complexes displaying a C_n axis with $n \geq 3$, although extension is possible. Axial symmetry can be a real, intrinsic property of the complex geometry or can derive from a dynamic process. To make evident the use of pseudocontact shifts, we can recall the McConnell–Robertson equation for axial complexes [3,4]:

$$\delta^{PC}_{Ln}(i) = \mathcal{D}_{Ln}\frac{3\cos^2\theta_i - 1}{r_i^3} = \mathcal{D}_{Ln}G(i) \quad (3)$$

Thus, the geometrical factor for *i*, $G(i)$, is a function of r_i (the length of the vector adjoining the nucleus *i* and the lanthanide) and of θ_i (the angle between this vector and the C_n axis). The constant $\mathcal{D}_{Ln}$ is characteristic of the complex and in particular depends on the lanthanide ion, the ligand structure, and the coordination polyhedron, as we shall see below.

As discussed previously for FC, PCS also follow a known trend from one lanthanide to another, provided isostructurality is preserved. This is because, following Bleaney's theory [23], $\mathcal{D}_{Ln}$ is proportional to the crystal field parameter B_0^2 through a constant, C_{Ln} which depends on the lanthanide. Even according to more sophisticated treatments, such as the one by Mironov et al. [24], the magnetic anisotropy and hence $\mathcal{D}_{Ln}$ can be written as

$$\mathcal{D}_{Ln} = C_{Ln} \cdot B \quad (4)$$

where *B* contains a sum of crystal field parameters of various orders.

The two parameters $\langle S_z\rangle_{Ln}$, C_{Ln} and their ratio are tabulated in several Refs. [2,4,17] and reproduced here in Table 1.

Thus both FC and PCS can be factorized in a lanthanide-dependent and a nucleus-dependent term and this offers an easy way to separate the two contributions to the total paramagnetic shift, according to the following equations, known as the Reilley method [9,17]. By inserting Eqs. (2), (3) and (4) into (1), we obtain

$$\delta^{para}_{Ln}(i) = \delta^{con}_{Ln}(i) + \delta^{PC}_{Ln}(i) = \langle S_z\rangle_{Ln} \cdot F(i) + C_{Ln} \cdot B \cdot G(i) \quad (5)$$

Provided the complexes are isostructural through some subset of the Ln series and that there are no major variations in the crystal field parameters collectively represented by B, we can write

$$\frac{\delta_{\mathrm{Ln}}^{\mathrm{para}}(i)}{\langle S_z\rangle_{\mathrm{Ln}}} = F(i) + \frac{C_{\mathrm{Ln}}}{\langle S_z\rangle_{\mathrm{Ln}}} B \cdot G(i) \tag{6}$$

Having observed that $\langle S_z\rangle_{\mathrm{Ln}}$ and C_{Ln} are known, a plot of $\delta_{\mathrm{Ln}}^{\mathrm{para}}(i)/\langle S_z\rangle_{\mathrm{Ln}}$ vs. $C_{\mathrm{Ln}}/\langle S_z\rangle_{\mathrm{Ln}}$ yields a straight line with slope and intercept

$$M^{\mathrm{Reilley}} = B \cdot G(i) \tag{7}$$

$$Q^{\mathrm{Reilley}} = F(i) \tag{8}$$

Accordingly, one can calculate PCS and FC for any lanthanide as

$$\delta_{\mathrm{Ln}}^{\mathrm{PC,\ Reilley}}(i) = M^{\mathrm{Reilley}}(i) \cdot C_{\mathrm{Ln}} \tag{9}$$

$$\delta_{\mathrm{Ln}}^{\mathrm{con,\ Reilley}}(i) = Q^{\mathrm{Reilley}}(i) \cdot \langle S_z\rangle_{\mathrm{Ln}} \tag{10}$$

Some discrepancies in this separation have been attributed to minor changes in the crystal field parameters e.g. due to the fact that lanthanide contraction brings about a shortening of the distances between Ln and the donor atoms on the ligand and a consequent geometry adjustment. This can be taken care of by means of the so-called three nuclei method which avoids the assumption of constant B [17].

The Reilley method gives reliable results for PCS, while for extracting good FC a modified approach may perform better. In this case, one divides both sides of Eq. (5) by C_{Ln} instead of $\langle S_z\rangle_{\mathrm{Ln}}$. For a detailed description, refer to Piguet and Geraldes's review: we shall ignore this method here because our objective is to extract good PCS.

Axial coordination of water or of some other ancillary ligand introduces a much greater source of variation of B. The contribution to the crystal field parameters of an axial ligand, B^{ax}, is limited to the terms B_0^n and is additive to those stemming from the other (non axial) ligands, B^{lig} [25]. We can thus write the following partition

$$B = B^{\mathrm{lig}} + B^{\mathrm{ax}} \tag{11}$$

Consequently the magnetic anisotropy term can be written as the sum [25,26]

$$D_{\mathrm{Ln}} = C_{\mathrm{Ln}}(B^{\mathrm{lig}} + B^{\mathrm{ax}}) = D_{\mathrm{Ln}}^{\mathrm{lig}} + D_{\mathrm{Ln}}^{\mathrm{ax}} \tag{12}$$

It is very common that for a given ligand early lanthanides yield hydrated complexes on account of their preference for higher coordination numbers, while late lanthanides provide anhydrous complexes. Thus, instead of being constant or following a regular trend over the series, B may display a more or less abrupt change, which often occurs around the middle of the transition and is called gadolinium break [18]. This corresponds to a rigid picture, where the complex is either totally hydrated (viz. fully occupied at the axial coordination site) or totally anhydrous, which is unfit to represent a dynamic situation.

The axial coordination site is often labile and this is a key feature of lanthanide complexes. Indeed, dynamic axial coordination is at the basis of functional systems, such as those quoted in the introduction, which must exchange axial ligands very rapidly. From the point of view of NMR spectroscopy, this means that the hydrated (H) and anhydrous (A) forms (plus water or in general any other ancillary ligand, W) must be in *fast exchange*, that is the rate of the equilibrium

$$\mathrm{H} \underset{k_-}{\overset{k_+}{\rightleftarrows}} \mathrm{A} + \mathrm{W} \tag{13}$$

is likely to be great compared to the shift difference (in Hz) between the corresponding nuclei in H and A. In this situation one cannot observe the spectra of the individual forms, but one set of resonances, at shifts

$$\delta_{\mathrm{Ln}}^{\mathrm{obs}}(i) = x_{\mathrm{Ln}}^{\mathrm{H}} \cdot \delta_{\mathrm{Ln}}^{\mathrm{H}}(i) + x_{\mathrm{Ln}}^{\mathrm{A}} \cdot \delta_{\mathrm{Ln}}^{\mathrm{A}}(i) = x_{\mathrm{Ln}} \cdot \delta_{\mathrm{Ln}}^{\mathrm{H}}(i) + (1 - x_{\mathrm{Ln}}) \cdot \delta_{\mathrm{Ln}}^{\mathrm{A}}(i) \tag{14}$$

where $x^{\mathrm{A}} = (1 - x)$ and $x^{\mathrm{H}} = x$ are the mole fractions of A and H for the complex with Ln.

It is thus reasonable to assume that to a first approximation PCS display the greatest sensitivity to the occupancy of the axial site, because they respond to the total charge distribution through $\mathcal{D}$, while the diamagnetic shift and FC are mostly local properties, depending primarily on the electron density and on unpaired electron delocalization. Therefore we shall write

$$\delta_{\mathrm{Ln}}^{\mathrm{obs}}(i) = \delta^{\mathrm{dia}}(i) + \delta_{\mathrm{Ln}}^{\mathrm{FC}}(i) + [x_{\mathrm{Ln}} \cdot \delta_{\mathrm{Ln}}^{\mathrm{PC,H}}(i) + (1 - x_{\mathrm{Ln}}) \cdot \delta_{\mathrm{Ln}}^{\mathrm{PC,A}}(i)] \tag{15}$$

and

$$\delta_{\mathrm{Ln}}^{\mathrm{para}}(i) = \delta_{\mathrm{Ln}}^{\mathrm{FC}}(i) + [x_{\mathrm{Ln}} \cdot \delta_{\mathrm{Ln}}^{\mathrm{PC,H}}(i) + (1 - x_{\mathrm{Ln}}) \cdot \delta_{\mathrm{Ln}}^{\mathrm{PC,A}}(i)] \tag{16}$$

Taking advantage of Eq. (12), we can write

$$\begin{aligned} \delta_{\mathrm{Ln}}^{\mathrm{PC,H}}(i) &= [\mathcal{D}_{\mathrm{Ln}}^{\mathrm{lig}} + \mathcal{D}_{\mathrm{Ln}}^{\mathrm{ax}}]G_i \\ \delta_{\mathrm{Ln}}^{\mathrm{PC,A}}(i) &= \mathcal{D}_{\mathrm{Ln}}^{\mathrm{lig}} G_i \end{aligned} \tag{17}$$

which combine in the term in square parentheses of Eq. (16) to

$$\begin{aligned} \delta_{\mathrm{Ln}}^{\mathrm{PC,tot}}(i) &= x_{\mathrm{Ln}} \cdot \delta_{\mathrm{Ln}}^{\mathrm{PC,H}}(i) + (1 - x_{\mathrm{Ln}}) \cdot \delta_{\mathrm{Ln}}^{\mathrm{PC,A}}(i) \\ &= [\mathcal{D}_{\mathrm{Ln}}^{\mathrm{lig}} + x_{\mathrm{Ln}} \cdot \mathcal{D}_{\mathrm{Ln}}^{\mathrm{ax}}]G_i = \mathcal{D}_{\mathrm{Ln}}^{\mathrm{tot}} G_i \end{aligned} \tag{18}$$

with

$$\mathcal{D}_{\mathrm{Ln}}^{\mathrm{tot}} = \mathcal{D}_{\mathrm{Ln}}^{\mathrm{lig}} + x_{\mathrm{Ln}} \cdot \mathcal{D}_{\mathrm{Ln}}^{\mathrm{ax}} \tag{19}$$

This demonstrates that $\mathcal{D}_{\mathrm{Ln}}^{\mathrm{tot}}$ is a function of the lanthanide not only through Bleaney's constant C_J but also because of variable occupancy of the axial site through x_{Ln}. Consequently, $\mathcal{D}_{\mathrm{Ln}}^{\mathrm{tot}}$ may not follow the expected trend and Reilley method for separating Fermi contact and pseudocontact shifts may fail.

The so-called two-nuclei method for separating FC and PCS terms is designed to take care of the variation in crystal field parameters along the series [17]. It has been proposed for the small variations in B induced by lanthanide contraction, but may very well serve to eliminate the problem of variable coordination number outlined above. An exhaustive account of the principles and applications of this method can be found elsewhere: here we shall just recall that it is based on the clever use of the paramagnetic shift values of a pair of nuclei on two isostructural complexes with different Ln^{3+} ions [17].

3. Two-lanthanides method

If we could neglect Fermi contact shifts altogether, by plotting $\delta_{\mathrm{Ln1}}^{\mathrm{para}}(i)$ vs. $\delta_{\mathrm{Ln2}}^{\mathrm{para}}(i)$ for two different isostructural complexes with lanthanides Ln1 and Ln2, we would obtain a straight line passing through the origin (which is rigorously true for PCS). The slope of this line is equal to the ratio

$$m = \frac{\mathcal{D}_{\mathrm{Ln1}}}{\mathcal{D}_{\mathrm{Ln2}}} \tag{20}$$

In the case of no variation in axial coordination (i.e. with the identity $x_{\mathrm{Ln1}} = x_{\mathrm{Ln2}}$) or in the crystal field parameters B, the above equation would reduce to the predictable constant

$$m^{\mathrm{ideal}} = \frac{C_J(\mathrm{Ln1})}{C_J(\mathrm{Ln2})} \tag{21}$$

But this is not the case if $x_{\mathrm{Ln1}} \neq x_{\mathrm{Ln2}}$ with reference to Eq. (14) (or in general if $B_{\mathrm{Ln1}} \neq B_{\mathrm{Ln2}}$).

We can now take advantage of the following facts regarding Fermi contact shifts:

(1) they are usually scattered in sign and magnitude;
(2) they are usually small for nuclei distant more than 4 bonds from Ln^{3+};
(3) for nuclei closer than 4 bonds from Ln^{3+}, FC may be large, but most often PCS are also very large (because of the short distance).

These three points concur in determining that plots of $\delta^{para}_{Ln}(i)$ for Ln1 and Ln2 are often linear to a very good approximation, possibly with the exception of small and highly conjugated ligands. The slope m provides the ratio of the $\mathcal{D}$ parameters given in Eq. (20), while taking into account any variation in the crystal field parameters B, notably the part due to variable axial coordination. Now, we can recall Eq. (4) and substitute $m\mathcal{D}_{Ln2}$ for $\mathcal{D}_{Ln1}$ in Eq. (6)

$$\frac{\delta^{para}_{Ln1}(i)}{\langle S_z\rangle_{Ln1}} = F(i) + \frac{m\mathcal{D}_{Ln2}}{\langle S_z\rangle_{Ln1}}G(i) \tag{22}$$

$$\frac{\delta^{para}_{Ln2}(i)}{\langle S_z\rangle_{Ln2}} = F(i) + \frac{\mathcal{D}_{Ln2}}{\langle S_z\rangle_{Ln2}}G(i) \tag{23}$$

These two can be combined to yield the modified Reilley equation

$$\frac{\delta^{para}_{Ln2}(i)}{\langle S_z\rangle_{Ln2}} - \frac{\delta^{para}_{Ln1}(i)}{\langle S_z\rangle_{Ln1}} = \mathcal{D}_{Ln2}G(i)\left(\frac{1}{\langle S_z\rangle_{Ln2}} - \frac{m}{\langle S_z\rangle_{Ln1}}\right) \tag{24}$$

The final equations for calculating FC and PCS for the nucleus i in the complexes with Ln1 and Ln2 are

$$\delta^{PC}_{Ln1}(i) = m\left(\frac{(\delta^{para}_{Ln2}(i)/\langle S_z\rangle_{Ln2}) - (\delta^{para}_{Ln1}(i)/\langle S_z\rangle_{Ln1})}{(1/\langle S_z\rangle_{Ln2}) - (m/\langle S_z\rangle_{Ln1})}\right) \tag{25}$$

$$\delta^{con}_{Ln1}(i) = \delta^{para}_{Ln1}(i) - \delta^{PC}_{Ln1} \tag{26}$$

We must note that this procedure does not rely on any assumption regarding the geometry of the complex (it falls into the category of the "model free methods"), provided they are axially symmetrical [17,27], and moreover does not use any hypothesis on the degree of hydration (or bond to any other axial ligand) in the two complexes.

4. The "all lanthanides" method

As an alternative and an extension to the method outlined above, we can take advantage of a set of Ln^{3+}complexes simultaneously.

(1) We select a reference compound, which must be chosen for being the best characterized one (with the largest set of unambiguously assigned resonances) and that is endowed with a large C_J and $C_J/\langle S_z\rangle_{Ln}$ ratio (see Table 1): the best choices may be in this order, Yb, Pr, and Ce. From now on, this reference lanthanide will be called ref. We must plot all the $\delta^{para}_{Ln}(i)$ vs. the $\delta^{para}_{ref}(i)$, and fit them to lines passing through the origin, with slopes m_{Ln}. Any significant deviation from linearity means that: (a) the complexes with Ln and ref are not isostructural and (b) if this occurs more or less systematically, then large contact contributions must be envisaged. In both cases, the method cannot be applied.
(2) We build modified Reilley plots for each nucleus i as a function of Ln, by plotting

$$\frac{\delta^{para}_{Ln}(i)}{\langle S_z\rangle_{Ln}} \text{ vs. } \frac{m_{Ln}}{\langle S_z\rangle_{Ln}} \tag{27}$$

This must yield straight lines, because, by analogy with what was seen in the previous section,

$$\frac{\delta^{para}_{Ln}(i)}{\langle S_z\rangle_{Ln}} = F(i) + G(i)\cdot B\cdot C^{ref}_J\frac{m_{Ln}}{\langle S_z\rangle_{Ln}} \tag{28}$$

(3) The slope and intercept of these straight lines are for each nucleus

$$M_i = B\cdot C^{ref}_J\cdot G(i) \tag{29}$$

$$Q = F(i) \tag{30}$$

(4) We are now able to identify the PCS for each nucleus in each Ln-complex, by the simple operation

$$\delta^{PC}_{Ln}(i) = m_{Ln}\cdot M_i \tag{31}$$

and

$$\delta^{PC}_{ref}(i) = M_i \tag{32}$$

while the contact terms can be obtained again through Eq. (10).

As we shall see in the case of cryptate below, the choice of the reference compound affects the results of the procedure to a very moderate extent for the PCS.

5. Applications

We shall discuss below a few practical cases, mostly taken from the literature, which will hopefully clarify the above outlined procedures and show their scope, their merit and their limitations.

It should be stressed that our approach is only applicable to systems with a set of pseudocontact-shifted signals, because only this ensures a good linear fitting for deriving the slopes m which must substitute the C_J in the standard Reilley treatment Consequently, some small-size traditional ligands for Ln^{3+}, such as acetylacetonates or 1,3-oxydiacetate are not amenable to our procedure.

5.1. DOTAM

In spite of the enormous interest towards DOTA and its derivatives, mostly due to their applications in MRI, it is hard to find a complete set of experimental shifts throughout the series. In their comprehensive paper on the structure of Yb DOTA in solution, Aime, Botta and Ermondi showed the ^{1}H spectra of most Ln DOTA but did not provide figures for the shifts or their assignment [28]. The diethylamide derivative of DOTA, called DOTAM (1,4,7,10-tetrakis(N,N-diethylacetamido)-1,4,7,10-tetraazacyclododecane, Scheme 1) was thoroughly studied by Forsberg et al. in a paper containing the most complete separation of FC and PCS of this whole family of compounds [29].[1]

A standard Reilley analysis of the paramagnetic shifts consisting of the plots of $\delta^{para}_{Ln}(i)/\langle S_z\rangle_{Ln}$ vs. $C_{Ln}/\langle S_z\rangle_{Ln}$ is reported in Fig. 1. This shows that there is a reasonably good linearity, with the gross exception of Sm and Tm. The former element is characterized by very small paramagnetic shifts (see C_{Sm} and $\langle S_z\rangle_{Sm}$ in Table 1), whose exact quantification is consequently rather error-prone. Moreover, $\langle S_z\rangle_{Sm}$ is poorly estimated because it depends on a multiplet of energy levels very close to the fundamental one. The fact that this parameter is very small and that it is at the denominator of the quantities to be plotted in Reilley method has the effect of amplifying any uncertainty.

[1] Proton 1 corresponds to the "axial at side proton" (ax@s), proton 2 corresponds to the "equatorial at side" proton (eq@s), proton 3 corresponds to the "axial at corner" proton (ax@c) and proton 4 corresponds to the "equatorial at corner" proton (eq@c).

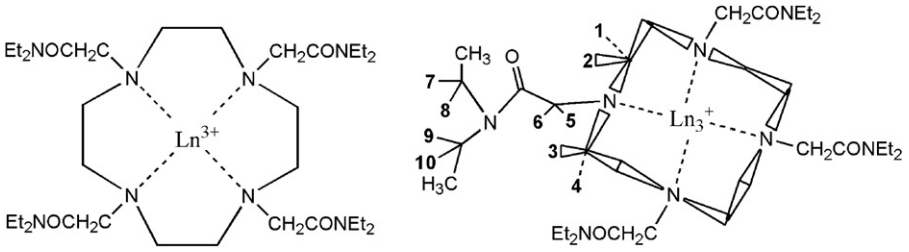

Scheme 1.

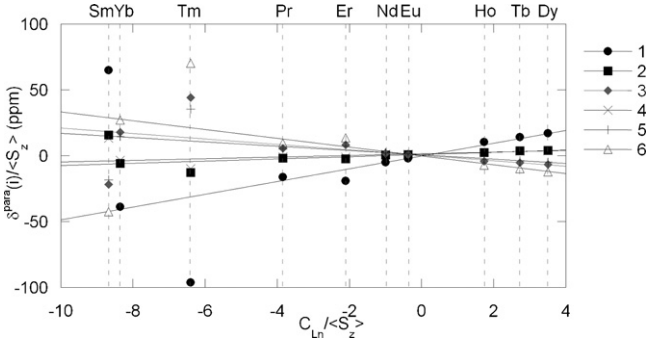

Fig. 1. Reilley plots for a selection of protons in Ln DOTAM. Data taken from Ref. [24].

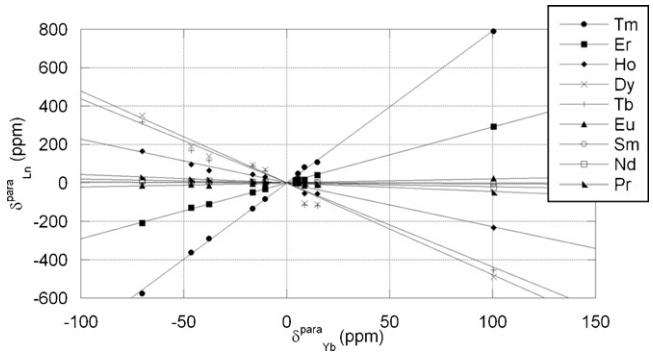

Fig. 2. Plots of $\delta^{para}_{Ln}(i)$ vs. $\delta^{para}_{Yb}(i)$, for Ln DOTAM.

To our understanding, there is no obvious reason for a deviation in Tm shifts, although they do often show exceptional behavior, as observed e.g. in Piguet and Geraldes's review [17].

By discarding the values for Tm and Sm, one can apply a linear fit to the Reilley plot for all protons in Ln DOTAM, obtaining the parameters shown in Table 2. Thereafter, one can achieve the separation of PCS and FC by means of Eqs. (9) and (10).

We can take two parameters to assess the quality of the Reilley method: the correlation coefficients $R(i)$ of the linear fit and the differences

$$\mathrm{diff}(i) = \delta^{para}_{Yb}(i) - (\delta^{PC,Reilley}_{Yb}(i) + \delta^{con,Reilley}_{Yb}(i)) \quad (33)$$

which should ideally be 0.

We can appreciate that the quality of Reilley plots for this set of complexes is very good, as witnessed by the correlation coefficients, which are all above 0.97 with the sole exceptions of H9 and H10. These two protons are remote from Ln and experience a particularly small paramagnetic shift. Moreover, they are geminal and their assignment throughout the series may be less safe than in the other cases.

Table 2
Slopes $M^{Reilley}(i)$, intercepts $Q^{Reilley}(i)$, and correlation coefficients $R^{Reilley}(i)$ of a linear fit of Reilley plots for Ln DOTAM, by excluding the data for Sm and Tm. The values of PCS and FC for Yb estimated through Eqs. (9) and (10) are reported in columns 5 and 6;the last column contains the difference defined in Eq. (33). PCS, FC and diff values are in ppm units.

Protons	$M^{Reilley}$	$Q^{Reilley}$	$R^{Reilley}$	PCS	FC	diff
1	4.85	−0.22	0.98	104.93	0.57	−4.90
2	0.84	0.99	0.97	18.23	−2.55	−0.78
3	−2.07	0.30	0.98	−44.75	−0.78	−0.87
4	0.62	1.45	0.98	13.35	−3.76	−0.89
5	−1.62	0.78	0.98	−35.14	−2.03	−0.43
6	−3.35	−0.13	0.98	−72.58	0.35	2.03
7	−0.84	−0.06	0.98	−18.11	0.15	1.55
8	−0.56	−0.07	0.98	−12.15	0.19	1.66
9	0.17	0.15	0.53	3.72	−0.39	2.27
10	0.06	−0.17	0.29	1.34	0.44	2.62

Table 3
Slopes m and correlation coefficients R of the linear fits (forced through the origin) shown in Fig. 2.

Lanthanide	m_{Ln}	R
Pr	−0.435	0.99
Nd	−0.19	0.86
Sm	−0.036	0.98
Eu	0.20	0.78
Tb	−4.37	0.98
Dy	−4.79	0.99
Ho	−2.27	0.99
Er	2.90	0.99
Tm	7.93	0.99

According to our method, we must take one complex as the reference and we choose Yb DOTAM. We plot the paramagnetic shifts for all protons in Ln DOTAM vs. those of the reference compound, obtaining plots as shown in Fig. 2, while the parameters of the linear fits (forced through the origin) are reported in Table 3.[2] The good linearity confirms that the complexes are isostructural and that the contributions of FC to the total paramagnetic shifts are small and scattered in sign and magnitude, as postulated in the previous sections. It is worth observing that also Tm provides a linear fit with Yb and it will be used in the following procedure, while it had to be arbitrarily discarded in the Reilley method.

We can now build plots of $\delta^{para}_{Ln}(i)/\langle S_z\rangle_{Ln}$ vs. $m_{Ln}/\langle S_z\rangle_{Ln}$ for each nucleus i, which yields the results shown in Fig. 3 and in Table 4.

In this case the slope M of our modified Reilley plots coincides by definition with the PCS of the reference compound (in this case Yb DOTAM).

The improvement over the conventional Reilley method is apparent from both quality parameters (R and diff), although in the present case the gain is only marginal: we had already found excellent linearity in Reilley plots, which could hardly be improved.

[2] We can appreciate that the values of the slopes m_{Ln} follow the same trend of the constants C_{Ln}, apart for Sm and Tm. This is consistent with the previous observation that Reilley plots are linear.

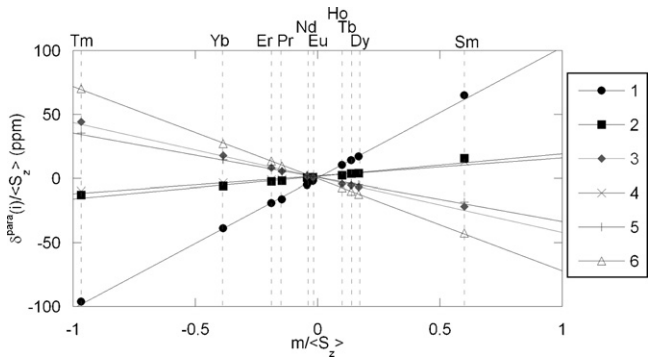

Fig. 3. Plots of $\delta^{para}_{Ln}(i)/\langle S_z\rangle_{Ln}$ vs. $m_{Ln}/\langle S_z\rangle_{Ln}$ for Ln DOTAM, having taken Yb DOTAM as the reference compound for calculating m_{Ln}.

Table 4
Slopes (M_i), intercepts (Q_i) and correlation coefficients (R_i) of modified Reilley plots for Ln DOTAM shown in Fig. 3. PCS and FC for the reference compound, Yb DOTAM, were calculated from the values of M_i and Q_i, respectively, according to Eqs. (31) and (10). The quality parameter diff is defined in Eq. (33). PCS, FC and diff values are in ppm units.

Protons	M	Q	R	PCS	FC	diff
1	102.21	0.54	1.00	102.21	−1.41	−0.20
2	17.60	1.73	0.98	17.60	−4.48	1.78
3	−42.80	0.09	1.00	−42.80	−0.24	−3.37
4	14.06	2.08	0.98	14.06	−5.39	0.03
5	−34.49	1.02	1.00	−34.49	−2.63	−0.48
6	−71.99	−0.09	1.00	−71.99	0.23	1.55
7	−17.57	−0.20	1.00	−17.57	0.53	0.65
8	−11.77	−0.32	0.99	−11.77	0.83	0.64
9	4.67	−0.08	0.87	4.67	0.21	0.72
10	−2.96	−1.27	0.47	−2.96	3.29	4.07

5.2. Cryptate

In 1999 Geraldes and coworkers reported a complete analysis of the paramagnetic shifts in a Ln cryptate derived from the condensation of tris(2-aminoethyl)amine and 2,6-diformylcresol [19], shown in Scheme 2. These authors highlighted a break in the Reilley

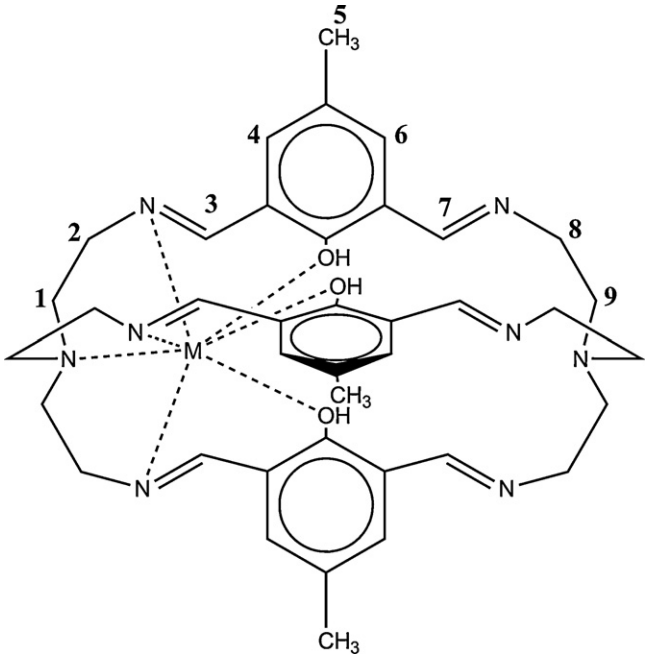

Scheme 2.

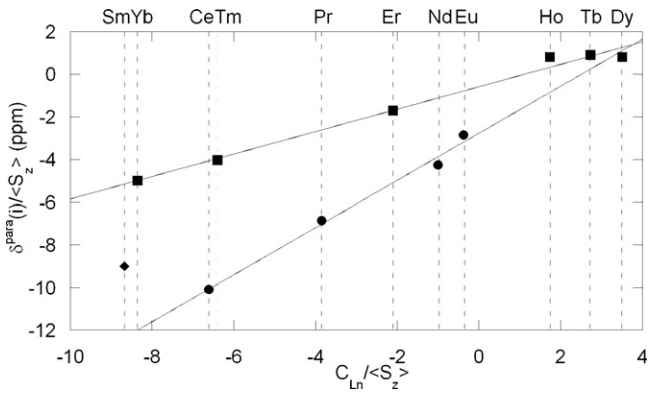

Fig. 4. Reilley plot for H3 in the series of cryptates depicted in Scheme 2. Data taken from Ref. [19].

plots, which was attributed to the presence of a coordinated water molecule in the first part of the transition, absent in the second part. This is particularly evident in the case of proton H3, as shown in Fig. 4.

In such a case it is clear that a conventional treatment through Reilley plots is only possible by treating separately early and late elements. This reduces the set of data and may worsen the quality of the analysis. Unfortunately, for the other protons in the very same molecule the situation is somewhat less evident, to the point that in some cases it would be difficult to put the break point to a specific lanthanide.

To use our modified method, we follow the same steps outlined in the previous section. We choose Pr as the reference compound, because it has an optimal ratio $C_{Ln}/\langle S_z\rangle$ (Table 1) and it is completely characterized, unlike the Yb derivative. We plot $\delta^{para}_{Ln}(i)$ vs. $\delta^{para}_{Pr}(i)$ and fit them with lines (passing through the origin), which leads to the results summarized in Table 5.

The correlation coefficients are satisfactory (although not always excellent), which demonstrates isostructurality through the series and small contributions of FC. The slopes m_{Ln} can be used to achieve the separation of PCS and FC following the sequence of operations described in Eqs. (31) and (10) with the results shown in Table 6.

Interestingly, by choosing Ce instead of Pr as the reference compound, we obtain PCS values differing by less than 10%, as shown in Supplementary material, Table S1.

Proof of the quality of our results is provided in Fig. 5, where we show the modified-Reilley plot for H3. Moreover, in Fig. 6 we report PCS and FC for the Pr complex calculated with our method compared to those of the original paper. We can simultaneously use all the available data, without any more or less arbitrary partition due to the gadolinium break, which is at variance with what was reported in the original paper.

Table 5
Slopes m and correlation coefficients R of the linear fits (forced through the origin) relative to the set of Ln cryptates of Ref. [19].

Lanthanide	m_{Ln}	R
Ce	0.67	0.96
Nd	0.59	0.86
Sm	0.0014	0.16
Eu	−0.60	0.35
Tb	4.94	0.64
Dy	3.64	0.66
Ho	2.00	0.76
Er	−1.73	0.95
Tm	−2.40	0.91
Yb	−1.10	0.81

Table 6
Slopes (M_i), intercepts (Q_i) and correlation coefficients (R_i) of modified Reilley plots for the Ln cryptates of Scheme 2. PCS and FC for the reference Pr cryptate, were calculated from the values of M_i and Q_i, respectively, according to Eqs. (31) and (10). The quality parameter diff is defined in Eq. (33). PCS, FC and diff values are in ppm units.

Protons	M	Q	R	PCS	FC	diff
H1ax	21.86	−1.23	0.94	21.86	−3.65	−5.22
H1eq	17.38	−1.24	0.98	17.38	−3.68	−0.67
H2ax	0.53	−0.72	0.36	0.53	−2.14	−0.17
H2eq	0.14	−0.38	0.13	0.14	−1.13	−0.70
H3	−10.79	−2.14	0.73	−10.79	−6.36	−3.23
H4	−8.84	2.16	0.45	−8.84	6.42	−3.22
H5	−2.18	0.36	0.65	−2.18	1.07	−0.68
H6	−1.71	0.03	0.94	−1.71	0.09	−0.21
H7[a]	8.24	−3.44	0.58	8.24	−10.22	2.96
H8ax	7.47	−0.45	0.99	7.47	−1.34	−0.46
H8eq	5.71	−0.36	0.99	5.71	−1.07	−0.32
H9ax	3.70	−0.24	0.99	3.70	−0.71	−0.17
H9eq	4.96	−0.31	0.99	4.96	−0.92	−0.35

[a] The values of δ^{para} (H7) are very small (below 1 ppm), consequently they are affected by a big error and should be considered unreliable.

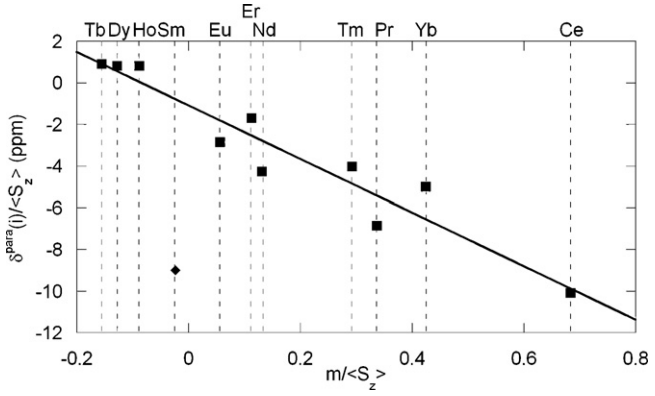

Fig. 5. Modified Reilley plot for H3 in the series of cryptates depicted in Scheme 2 after the treatment proposed in this work.

Although some of the correlation coefficients of the plots $\delta^{para}_{Ln}(i)$ vs. $\delta^{para}_{Pr}(i)$ are unusually small compared to other cases, this does not prevent a satisfactory extraction of PCS, which are in close agreement with those found in Ref. [19].

5.3. Saá's Binolam complexes

At first sight, the complexes shown in Scheme 3, introduced by Saá [30–33], are very similar to the well known Shibasaki's

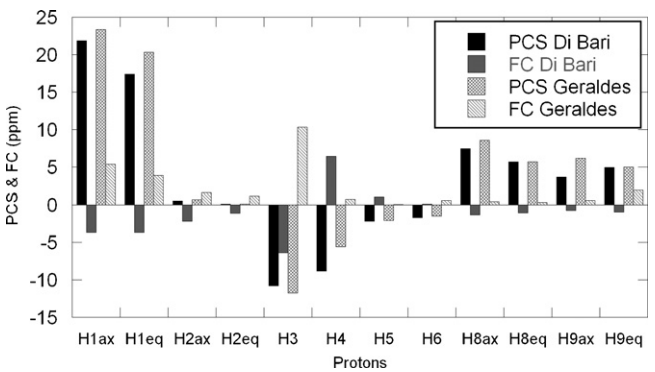

Fig. 6. Comparison between PCS and FC for PR cryptate, calculated according to our method and extrapolated from the data of Ref. [19].

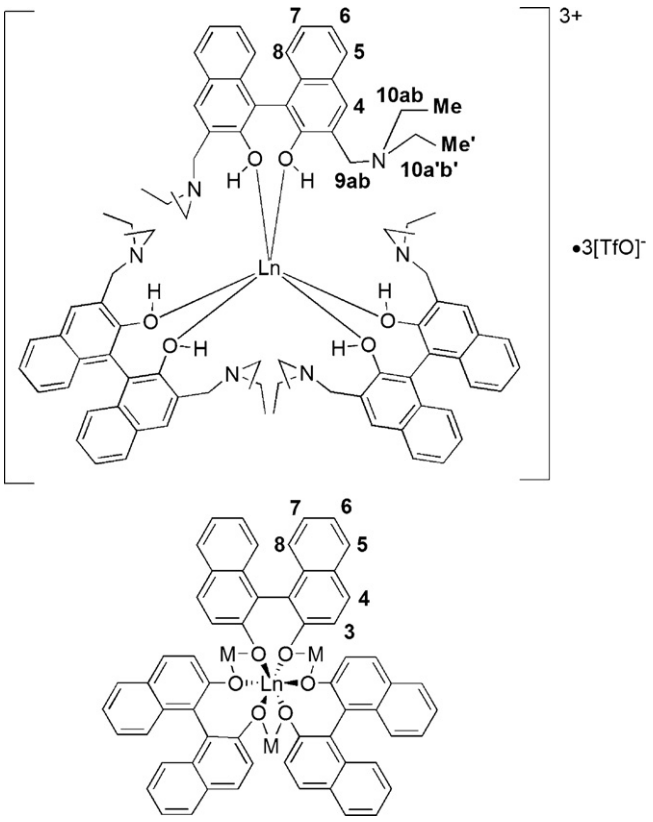

Scheme 3.

heterobimetallic systems treated below. The difference consists of the incorporation of a Brønsted base proximal to the naphthol hydroxyl. As a consequence, complex formation does not require the treatment with a base, which is a necessary step in Shibasaki's systems, and the result is a set of alkali metal-free (monometallic) compounds, displaying completely different structural and chemical properties [33]. The only system which led to crystals amenable for XRD was the Sc complex, while heavier elements were reluctant to crystallize.

The accurate analysis of paramagnetic shifts for Pr, Nd and Yb complexes unambiguously demonstrated isostructurality throughout the series, at least in the sense that the geometrical factors $G_{Ln}(i)$ are equal [33]. The existence of a dynamic hydration equilibrium becomes apparent through very simple experiments, where the sample water content is changed: the paramagnetic shifts of all nuclei are water sensitive to a more or less marked extent, as a function of Ln. One observes greater variations of the ^{1}H shifts for Pr and Nd Binolam, and much smaller for the Yb derivative. Thus, this system falls very obviously into the case depicted in Eq. (19), i.e. one set of $G_{Ln}(i)$, but water-dependent $\mathcal{D}$.

Linearity of the plots $\delta^{para}_{Ln}(i)$ vs. $\delta^{para}_{Yb}(i)$ was already observed in Ref. [33], where it was also observed that the slopes m_{Ln} are very far from what was expected from Bleaney's factors. Accordingly, separation of FC and PCS cannot be attempted by means of the standard Reilley method but can be achieved successfully by our two-lanthanides method, through Eqs. (25) and (26), with the results reported for the Pr–Nd couple in Table 7 and for the Pr–Yb one in Table 8.

We can appreciate the consistency of the FC terms calculated for different Ln and also that they are small, on account of the limited possibility of delocalization of unpaired spin density over the moderately large ligand.

Table 7
Separation of PCS and FC according to the two-lanthanides method for Ln Binolam for the couple Pr–Nd. Para, PCS and FC values are in ppm units.

Protons	Pr			Nd		
	Para	PCS	FC	Para	PCS	FC
4	−0.76	−0.81	0.05	1.05	0.97	0.08
5	−0.49	−0.44	−0.05	0.46	0.53	−0.07
6	−0.33	−0.25	−0.08	0.17	0.30	−0.13
7	−0.19	−0.27	0.08	0.45	0.33	0.12
8	−0.67	−0.76	0.09	1.04	0.91	0.13
9a	−1.12	0.03	−1.15	−1.77	−0.03	−1.74
9b	−2.06	−1.33	−0.73	0.49	1.59	−1.10
10a	1.84	1.89	−0.05	−2.35	−2.27	−0.08
10b	1.54	1.51	0.03	−1.78	−1.82	0.04
10a′	0.33	0.44	−0.11	−0.69	−0.53	−0.16
10b′	0.58	0.42	0.16	−0.26	−0.50	0.24
Me	0.72	0.59	0.13	−0.52	−0.71	0.19
Me′	0.54	0.57	−0.03	−0.73	−0.68	−0.05

5.4. Shibasaki's heterobimetallic catalysts

Shibasaki introduced a class of C_3-symmetric Ln complexes based on binaphtholate (hereafter Binolate) as the ligand, which raised a great interest because of their properties as enantioselective catalysts in a number of organic reactions (Scheme 3) [34]. As for many other catalysts, the possibility of coordination of ancillary ligands is of prime importance, since this dynamic binding is at the basis of substrate activation.

The complexes of formula $M_3Ln(Binolate)_3$ (M = Li, Na, K) display a pinwheel structure, which has been investigated in great detail both in solution and in the solid state [35]. In the latter case, single crystal XRD demonstrates that early elements provide hydrated complexes, while late elements yield anhydrous ones. Notably, for Eu, both forms have been reported. In solution, the investigation into hydration number is more difficult and only indirect proofs have been provided. By two different synthetic procedures, Aspinall et al. [36] and Walsh et al. [37] obtained two completely different sets of ^{1}H NMR data for what is apparently the very same complex: $Li_3Eu(Binolate)_3$. This must be attributed to the different extents of hydration in the two compounds, since in only one case (Aspinall) was the sample obtained in rigorously water-free conditions. Interestingly, no-one reports on the existence of two sets of signals for hydrated and anhydrous forms: we must conclude that this system falls into the fast exchange regime, as envisaged in Eqs. (13)–(19) and that the Reilley analysis would lead to inconsistent results.

Unlike in the cases discussed above and notwithstanding the large interest and the numerous reports on heterobimetallic complexes, in the literature we were able to find ^{1}H shifts only for a limited number of lanthanides. Usually the water content of the various samples is difficult to estimate and moreover, they refer to different alkali metals M.

Table 8
Separation of PCS and FC according to the two-lanthanides method for Ln Binolam for the couple Pr–Yb. Para, PCS and FC values are in ppm units.

Protons	Pr			Yb		
	Para	PCS	FC	Para	PCS	FC
4	−0.76	−0.92	0.16	−4.52	−4.38	−0.14
5	−0.49	−0.52	0.03	−2.51	−2.48	−0.03
6	−0.33	−0.39	0.06	−1.92	−1.87	−0.05
7	−0.19	−0.31	0.12	−1.57	−1.47	−0.10
8	−0.67	−0.97	0.30	−4.88	−4.62	−0.26
9a	−1.12	−0.91	−0.21	−4.16	−4.34	0.18
9b	−2.06	−1.51	−0.55	−6.72	−7.20	0.48
10a	1.84	1.77	0.07	8.38	8.44	−0.06
10b	1.54	1.63	−0.09	7.82	7.74	0.08
10a′	0.33	0.64	−0.31	3.33	3.06	0.27
10b′	0.58	0.55	0.03	2.61	2.63	−0.02
Me	0.72	0.62	0.10	2.88	2.96	−0.08
Me′	0.54	0.82	−0.28	4.13	3.89	0.24

Table 9
Separation of PCS and FC according to the two-lanthanides method for $Li_3Pr(Binolate)_3$ vs. those of $Li_3Yb(Binolate)_3$. Para, PCS and FC values are in ppm units.

Protons	$Li_3Pr(Binolate)_3$			$Li_3Yb(Binolate)_3$		
	Para	PCS	FC	Para	PCS	FC
3	−18.51	−19.29	0.78	83.20	83.88	−0.68
4	−4.03	−3.68	−0.35	16.29	15.98	0.31
5	0.86	−0.58	1.44	1.26	2.51	−1.25
6	1.44	0.85	0.59	−4.21	−3.70	−0.51
7	2.97	1.66	1.31	−8.37	−7.23	−1.14
8	6.64	4.61	2.03	−21.82	−20.05	−1.77

As we said, Pr and Yb surely display opposite behavior: one should mostly yield the water-capped complexes, the other should provide the anhydrous ones. We proceed through our modified method: first of all, we plot all the paramagnetic shifts for $Li_3Pr(Binolate)_3$ vs. those of $Li_3Yb(Binolate)_3$, and we obtain the slope

$$m_{Pr,Yb} = -0.23 \tag{34}$$

which is far from the ideal value of $m^{ideal} = -0.52$ (see Eq. (21)), on account of the different hydration states of the two species. By application of Eqs. (25) and (26), we obtain the PCS and FC reported in Table 9. We can appreciate that the FC terms are small for most nuclei.

In the same way, we can treat both sets of data for $Li_3Eu(Binolate)_3$, as reported by Aspinall and Walsh, which are very different, comparing their paramagnetic shifts with those of $Li_3Yb(Binolate)_3$ method and we find

$$\begin{aligned} m_{Eu\ Aspinall,Yb} &= 0.07 \\ m_{Eu\ Walsh,Yb} &= 0.22 \end{aligned} \tag{35}$$

This allows us to use the two-lanthanides method and to obtain the PCS and FC reported in Table 10. A general comment for all these cases is that the FC terms are in any case small for most nuclei.

These heterobimetallic systems feature another aspect, which is particularly interesting for our analysis. The alkali metal has the effect of modulating the charge on the Binolate oxygen atoms and consequently of changing the crystal field parameters, while leaving the overall geometry of the various complexes unchanged, as observed by Aspinall and subsequently confirmed [35,36]. This means that the corresponding nuclei on complexes with different M and/or different hydration numbers have the same set of $G(i)$. This observation prompted us to put forward another more venturous attempt: using sets of data of heterogeneous systems, i.e. separate PCS and FC from systems which differ not only in the Ln but also in the alkali metal M. Accordingly, we pursued the two-lanthanides method on the data of $Li_3Pr(Binolate)_3$ vs. of $Na_3Yb(Binolate)_3$ [35]. The results are reported in Table 11 and compare very well

Table 10
Separation of PCS and FC according to the two-lanthanides method for the two sets of data relative to the formula $Li_3Eu(Binolate)_3$ taken from Ref. [37] (Walsh) and from Ref. [36] (Aspinall), vs. those of $Li_3Yb(Binolate)_3$. Para, PCS and FC values are in ppm units.

Protons	Eu Walsh			Eu Aspinall		
	Para	PCS	FC	Para	PCS	FC
3	17.91	18.33	−0.42	5.17	6.09	−0.92
4	3.10	3.61	−0.51	1.62	1.18	0.44
5	0.58	0.26	0.32	1.83	0.06	1.77
6	−0.72	−0.94	0.22	1.23	−0.34	1.57
7	−3.05	−1.77	−1.28	−0.92	−0.61	−0.31
8	−7.16	−4.67	−2.49	−4.66	−1.54	−3.12

Table 11
Results of the separation of PCS and FC according to the two-lanthanides method mixing data relative to two different alkali metals in heterobimetallic systems: $Li_3Pr(Binolate)_3$ vs. of $Na_3Yb(Binolate)_3$. Para, PCS and FC values are in ppm units.

Protons	$Li_3Pr(Binolate)_3$			$Na_3Yb(Binolate)_3$		
	Para	PCS	FC	Para	PCS	FC
3	−18.51	−19.87	1.36	36.3	37.48	1.18
4	−4.03	−3.34	−0.69	6.9	6.30	−0.60
5	0.86	−0.64	1.50	−0.1	1.21	1.31
6	1.44	1.03	0.41	−2.3	−1.94	0.36
7	2.97	1.00	1.97	−3.6	−1.88	1.72
8	6.64	3.16	3.48	−9	−5.97	3.03

to those of Table 9: the PCS and FC of $Li_3Pr(Binolate)_3$ separated taking the two Yb compounds as the reference are practically identical.

5.5. DOTMA

The most involved system we wish to treat is a complete lanthanide series of Ln DOTMA [38,39], a chiral DOTA analogue (DOTMA = 1,4,7,10-tetrakis(*R*)-methylacetic acid-1,4,7,10-tetraazacyclododecane), the all-*R* derivative structure is reported in Scheme 4.

Gd DOTA is one of the most widely used MRI contrast agents and this clearly demonstrates that hydration/dehydration equilibrium is a key feature. Water exchange has been studied with great accuracy for this parent compound and for a number of closely related ones [40]. Another relevant dynamic aspect consists of an equilibrium between two different conformations, leading to a square antiprismatic coordination (SAP) or a twisted square antiprismatic one (TSAP) [28,38,41,42]. These two forms are usually in slow exchange on the paramagnetic NMR timescale, as is clearly manifest by two distinct sets of signals in the ^1H spectra. Their mole proportion is variable throughout the series, and also their affinity for water is changeable. DOTA and DOTMA are formally very similar, the difference consisting of the fact that one hydrogen atom of the acetate arms of DOTA is substituted with a methyl group in DOTMA, which introduces a further element of chirality. A very striking feature of these molecules is that the PCS of TSAP and of SAP forms are proportional, on account of the practical (accidental) identity of the geometrical factors G_i for all nuclei [39,43]. This can be easily demonstrated by plotting the PCS (or even the paramagnetic shifts) of the two forms of the same Ln complex one against the other. Thus, in spite of the great geometrical detail attained by paramagnetic NMR, it may be difficult to recognize if one is dealing with one or the other form, for a new term of this family of compounds. On the other hand, TSAP and SAP feature relevant differences in their ability to bind water in the first coordination sphere and also in the dynamic exchange of bound and bulk water, which has relevant consequences in MRI [15,40,44].

Very commonly, the distinction between SAP and TSAP forms is based on the difference in the most downfield-shifted signals [26,45], due to protons occupying the axial "at the corner" position in the cyclen macrocycle [46], which amounts to saying that

$$|\mathcal{D}^{TSAP}| < |\mathcal{D}^{SAP}| \quad (36)$$

which is in agreement with Mironov's results for the deformation of the square antiprism [24]. Unfortunately, when only one set of signals is visible in the NMR spectrum the assignment may be less safe. Moreover, predicting the prevalence for TSAP or SAP may be very difficult, because of a subtle enthalpy/entropy compensation effect [39,41], and consequent interplay with even minor solvation or polarizability effects [45].

Table 12
Experimental ^1H NMR shifts (ppm) of Ln DOTMA (major and minor forms).

Protons	La	Lu	Ce		Pr	Nd		Sm		Eu		Tb		Ho		Er		Tm		Yb	
			Maj	Min	Maj	Maj	Min	Maj	Min	Maj	Min	Maj	Min	Maj	Min	Maj	Min	Maj	Min	Maj	Min
Ax@s	2.83	3.01	−13.35	−23.74	−33.00	−12.70	−26.7	−0.21	40.80	20.00	40.75	−367.20	−464.60	ND	ND	211	122.0	ND	327	96.43	
Eq@s	2.54	2.69	0.91	ND	1.14	4.46	1.7	ND	−10.40	−3.50	1.14	−85.60	−101.30	−39.22	−60.73	21.00	18.70	69.40	61.80	17.68	
Eq@c	2.78	2.69	0.17	−2.37	−1.44	7.02	ND	ND	−5.53	−8.83	−23.83	−88.00	−108.50	−43.39	−62.70	40.80	32.70	93.80	82.00	11.98	
M	1.25	1.20	3.60	ND	6.69	3.70	ND	1.75	−4.01	−1.74	−3.95	61.60	67.77	35.77	42.46	−43.70	−28.00	−104.0	−67.00	−14.68	
Ax@c	3.38	3.01	7.80	10.43	14.59	8.11	10.30	3.39	1.14	−4.01	−5.53	136.09	154.60	82.14	96.11	−106.5	−69.30	−255.9	−163	−21.53	
ac	3.91	3.91	14.83	21.72	29.17	13.41	23.65	6.63	−23.80	−8.41	−10.40	301.60	344.10	ND	ND	−211	−148.0	ND	−346	−69.94	

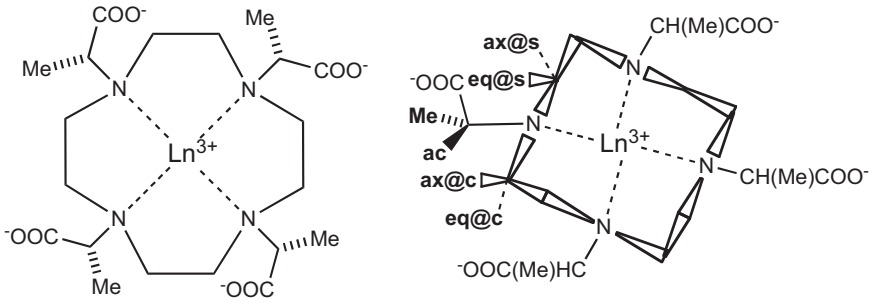

Scheme 4.

Lastly, a further complication arises from the fact that unexpected differences in the crystal field parameters for some elements, notably Tm and Er are observed [45].

The linear relation between PCS for the two forms, in the context of the present work, calls for another property: to a large extent a plot of $\delta^{para}_{Ln1}(i)$ vs. $\delta^{para}_{Ln2}(i)$ will provide a good linear fit not only independent of Ln1 and Ln2, but also independent of the fact that we are dealing with a TSAP or a SAP form.

To some extent, we may say we are in a situation similar to that described above for heterobimetallic catalysts, where we could take advantage of data arising from complexes with different alkali metals.

Separating FC from PCS in DOTMA (as well as in DOTA) is hardly possible by means of the standard Reilley method, because of the combined effect of the SAP/TSAP and of the hydration/dehydration equilibria. Nonetheless, we obtained excellent results using our modified method.

First of all, we choose as the reference spectrum the major form of Yb DOTMA (which is TSAP) and we plot all the shifts of both major and minor forms of the various Ln DOTMA (Table 12) vs. this set of data.

As we see from Table 13, the correlation coefficients are all fully satisfactory. The slopes of these linear fits can be used to build one modified Reilley plot for each proton, by taking into account simultaneously all of the available data for Ln DOTMA in both major and minor forms and to achieve separation of PCS and FC, as shown in Table 14.

We can appreciate that the quality of this separation is excellent, as measured by the difference of Eq. (33) for Yb DOTMA and also by the fact that the trend of FC follows reasonably closely the one found for the correspondent protons in Ln DOTAM.

Table 13
Slopes and correlation coefficients for linear fits (forced through the origin) for $\delta^{para}_{Ln1\,maj/min}(i)$ vs. $\delta^{para}_{Yb\,maj}(i)$.

Lanthanide	*m*	*R*
Ce	−0.16	0.99
Ce min	−0.26	0.97
Pr	−0.37	0.99
Nd	−0.15	0.92
Nd min	−0.29	0.98
Sm	−0.03	0.98
Eu	0.17	0.74
Eu min	0.30	0.75
Tb	−4.10	0.99
Tb min	−4.96	0.99
Ho	−3.04	0.98
Ho min	−3.86	0.96
Er	1.64	0.98
Er min	2.56	0.96
Tm	8.47	0.98
Tm min	4.10	0.95

Table 14
Slopes (equal to the PCS of Yb DOTMA), intercepts and correlation coefficients of modified Reilley plots for all protons in Ln DOTMA, obtained by taking the major form of Yb DOTMA as the reference spectrum; FC terms for Yb DOTMA calculated according to Eq. (10). The last column displays the quality parameters diff as in Eq. (33) for Yb DOTMA. PCS, FC and diff values are in ppm units.

Protons	*M*	*Q*	*R*	diff
Ax@s	89.12	0.23	0.99	4.90
Eq@s	10.66	0.51	0.94	5.66
Eq@c	13.14	0.23	0.95	−3.25
M	−13.65	0.18	0.99	−1.76
Ax@c	−30.83	0.34	0.98	7.17
ac	−79.54	−0.40	0.99	4.65

6. Conclusions

We here briefly reviewed the standard protocol for separating pseudocontact and contact terms from total paramagnetic shifts in lanthanide compounds, with particular reference to axial symmetry. We proposed a simple but not previously described modification of this protocol for compensating for any variation in crystal field parameters. We discussed the standard and modified protocols on four sets of NMR data taken from the literature and on an unreported set for a chiral derivative of Ln DOTA. We discussed the main limitation of standard protocol, consisting of the necessity to restrict the analysis to some lanthanides characterized by similar crystal field parameter(s). In many cases, the change in these parameters may be not trivial and sometimes even unpredictable, which introduces a certain degree of arbitrariness. This is especially true in cases of significant axial ligand dynamics, where capped and non-capped forms may coexist and freely exchange, as notably found in catalytic systems and in MRI contrast agents. The proposed analysis offers a new "lens", to extract the PCS from the total paramagnetic shifts. It has the merit of avoiding any more or less arbitrary partition into early and late lanthanides (or the notion of "gadolinium break") and can effortlessly and seamlessly cope with changes in crystal field parameters arising e.g. from axial dynamics or from lanthanide contraction. We cannot and do not claim that the PCS extracted in this way are *more accurate* than any other, because their "true" values are only experimentally accessible through a more or less questionable separation protocol. We only can say that they compare well with sets of geometrical factors arising from a structural optimization. In any case, however, there is some degree of self-reference which invalidates the comparison.

Our procedure can be classified in the context of "model free" methods, because it makes no assumption on a specific geometrical model and also avoids reference to Bleaney's constants. It can be used even if only a few (two) Ln derivatives of a certain complex are characterized, independent of the position of the elements in the series, i.e. early and late lanthanides can be analyzed simultaneously. One of the most interesting features of this new method is that we can even mix and treat together heterogeneous data,

which is especially relevant in some specific cases where it may be difficult to know for sure the nature of the species observed in solution, as in the case of the binaphtholate heterobimetallic systems or in the presence of different structural forms such as in the DOTA derivatives.

Appendix A. Supplementary data

Supplementary data associated with this article can be found, in the online version, at doi:10.1016/j.ccr.2011.05.010.

References

[1] I. Bertini, C. Luchinat, G. Parigi, R. Pierattelli, Dalton Trans. (2008) 3782.
[2] I. Bertini, C. Luchinat, Coord. Chem. Rev. 150 (1996).
[3] J.A. Peters, J. Huskens, D.J. Raber, Prog. NMR Spectrosc. 28 (1996) 283.
[4] L. Di Bari, P. Salvadori, Coord. Chem. Rev. 249 (2005) 2854.
[5] G. Pintacuda, M. John, X.C. Su, G. Otting, Acc. Chem. Res. 40 (2007) 206.
[6] X.C. Su, G. Otting, J. Biomol. NMR 46 (2010) 101.
[7] S. Cotton, Lanthanide and Actinide Chemistry, John Wiley & Sons, Ltd, 2006.
[8] J. Reuben, J. Magn. Reson. 50 (1982) 233.
[9] C.N. Reilley, B.W. Good, Anal. Chem. 47 (1975) 2110.
[10] R.S. Dickins, S. Aime, A.S. Batsanov, A. Beeby, M. Botta, J. Bruce, J.A.K. Howard, C.S. Love, D. Parker, R.D. Peacock, H. Puschmann, J. Am. Chem. Soc. 124 (2002) 12697.
[11] R.S. Dickins, A. Badari, Dalton Trans. (2006) 3088.
[12] M. Shibasaki, N. Yoshikawa, Chem. Rev. 102 (2002) 2187.
[13] J.-C.G. Bunzli, C. Piguet, Chem. Soc. Rev. 34 (2005) 1048.
[14] P. Caravan, Chem. Soc. Rev. 35 (2006) 512.
[15] M. Woods, E.W.C. Donald, A.D. Sherry, Chem. Soc. Rev. 35 (2006) 500.
[16] I. Persson, P. D'Angelo, S. De Panfilis, M. Sandstrom, L. Eriksson, Chem. Eur. J. 14 (2008) 3056.
[17] C. Piguet, C.F.G.C. Geraldes, in: J.K.A. Geschneidner, J.C.G. Bunzli, V.K. Pecharsky (Eds.), Handbook on the Physics and Chemistry of Rare Earths, Elsevier, 2003, p. 353.
[18] S. Rigault, C. Piguet, J. Am. Chem. Soc. 122 (2000) 9304.
[19] C. Platas, F. Avecilla, A. de Blas, C.F.G.C. Geraldes, T. Rodriguez-Blas, H. Adams, J. Mahia, Inorg. Chem. 38 (1999) 3190.
[20] R.J. Abraham, R. Koniotou, F. Sancassan, J. Chem. Soc. Perkin Trans. 2 (2002) 2025.
[21] L. Di Bari, M. Lelli, P. Salvadori, Chem. Eur. J. 10 (2004) 4594.
[22] R.M. Golding, M.P. Halton, Aust. J. Chem. 25 (1972) 2577.
[23] B. Bleaney, J. Magn. Reson. 8 (1972) 91.
[24] V.S. Mironov, Y.G. Galyametdinov, A. Ceulemans, C. Gorller-Walrand, K. Binnemans, J. Chem. Phys. 116 (2002) 4673.
[25] L. Di Bari, G. Pintacuda, P. Salvadori, R.S. Dickins, D. Parker, J. Am. Chem. Soc. 122 (2000) 9257.
[26] R.S. Dickins, D. Parker, J.I. Bruce, D.J. Tozer, Dalton Trans. (2003) 1264.
[27] A.G. Martynov, Y.G. Gorbunova, Polyhedron 29 (2010) 391.
[28] S. Aime, M. Botta, G. Ermondi, Inorg. Chem. 31 (1992) 4291.
[29] J.H. Forsberg, R.M. Delaney, Q. Zhao, G. Harakas, R. Chandran, Inorg. Chem. 34 (1995) 3705.
[30] J.M. Saá, F. Tur, J. Gonzalez, M. Vega, Tetrahedron Asymmetr. 17 (2006) 99.
[31] F. Tur, J.M. Saá, Org. Lett. 9 (2007) 5079.
[32] J.M. Saá, F. Tur, J. González, Chirality 21 (2009) 836.
[33] L. Di Bari, S. Di Pietro, G. Pescitelli, F. Tur, J. Mansilla, J.M. Saá, Chem. Eur. J. 16 (2010) 14190.
[34] M. Shibasaki, H. Sasai, T. Arai, Angew. Chem. Int. Ed. Engl. 36 (1997) 1236.
[35] L. Di Bari, M. Lelli, G. Pintacuda, G. Pescitelli, F. Marchetti, P. Salvadori, J. Am. Chem. Soc. 125 (2003) 5549.
[36] H.C. Aspinall, J.F. Bickley, J.L.M. Dwyer, N. Greeves, R.V. Kelly, A. Steiner, Organometallics 19 (2000) 5416.
[37] A.J. Wooten, P.J. Carroll, P.J. Walsh, J. Am. Chem. Soc. 130 (2008) 7407.
[38] H.G. Brittain, J.F. Desreux, Inorg. Chem. 23 (1984) 4459.
[39] L. Di Bari, G. Pintacuda, P. Salvadori, Eur. J. Inorg. Chem. (2000) 75.
[40] A. Borel, J.F. Bean, R.B. Clarkson, L. Helm, L. Moriggi, A.D. Sherry, M. Woods, Chem. Eur. J. 14 (2008) 2658.
[41] S. Aime, M. Botta, M. Fasano, M.P.M. Marques, C.F.G.C. Geraldes, D. Pubanz, A.E. Merbach, Inorg. Chem. 36 (1997) 2059.
[42] S. Hoeft, K. Roth, Chem. Ber. 126 (1993) 869.
[43] L. Di Bari, G. Pintacuda, P. Salvadori, J. Am. Chem. Soc. 122 (2000) 5557.
[44] F.A. Dunand, R.S. Dickins, D. Parker, A.E. Merbach, Chem. Eur. J. 7 (2001) 5160.
[45] T. Mani, G. Tircso, P.Y. Zhao, A.D. Sherry, M. Woods, Inorg. Chem. 48 (2009) 10338.
[46] L. Di Bari, G. Pescitelli, A.D. Sherry, M. Woods, Inorg. Chem. 44 (2005) 8391.